Structural Role of Strontium Oxide in Modified Silicate Glasses

Gomaa El-Damrawi (gomaaeldamrawi@gmail.com)
Mansoura University Faculty of Science https://orcid.org/0000-0001-9144-0682
Rawia Ramadan
National Research Centre
mohamed Biomey
Mansoura University Faculty of Science

Research Article

Keywords: Strucutr, Physical properties, glasses, Glass Ceramics

Posted Date: April 26th, 2021

DOI: https://doi.org/10.21203/rs.3.rs-443520/v1

Version of Record: A version of this preprint was published at Silicon on July 22nd, 2021. See the published version at https://doi.org/10.1007/s12633-021-01226-w.

Structural role of strontium oxide in modified silicate glasses.

G El Damrawi[1*], R.M. Ramadan[2] and M.A. Biomy[3]

[1,3]Glass Research Group, Physics Department, Faculty of Science, Mansoura University, Mansoura 35516, Egypt

[2] Microwave Physics and Dielectrics Department, Physics Research Division, National Research Centre, 12622, Dokki, Cairo, Egypt

Abstract

In the composition range of x= 0-15 mol%, glasses in the system $24.5Na_2O.24.5CaO.6P2O5.xSrO.(45\text{-}x)SiO_2$ have been studied. The glasses are transparent and have an amorphous network structure when they are as prepared. Heat treated glasses, on the other hand, are transformed into opaque white glass ceramics with a highly crystalline network structure. The main well-formed crystalline species in material bioactivity were apatite (calcium phosphate, $Ca_3(PO_4)_2$, wollastonite (calcium silicate, $CaSiO_3$), and strontium calcium phosphate [$Ca_2Sr(PO_4)_2$. Increasing SrO improves material crystallite and increases the host glass matrix's hardness. The modification of the apatit Ca(PO3)2 to involve Sr ions inducing Ca2Sr (PO4)2 apatite one is thought to be the cause of the change in XRD spectra, 31P NMR chemical shift, and hardness number as SrO increases. These species help to improve material properties and hardness.

Keywords **Strucutr, Physical properties, glasses, Glass Ceramics**

Corresponding author gomaaeldamrawi@gmail.com

1 Introduction

Porous inorganic materials have unique properties that can help biomaterials be developed for controlled loading stresses and/or the release of biologically active substances [1, 2]. Bioactive glasses, also known as glass ceramics, are any compatible material that can form a calcium phosphate interfacial layer that resembles the biological apatite found in bones [3,4] . Furthermore, bioactive glasses can actively stimulate bone

growth by releasing critical concentrations of ionic dissolution products, which cause rapid expression of genes that regulate osteogenesis and growth factor production[1, 5]. In this regard, strontium-based bioactive glasses have a strong ability to prevent osteoclasts from resorbing bone[6, 7]. SrO has recently been shown to improve the surface adhesion properties of strontium-containing glasses, resulting in increased material hardness.. The lower electronegativity of Sr ions in the glassy network compared to Ca2+ ions is thought to be the reason for the increased surface adhesion[8, 9]. Because of Sr's low electronegativity, a more balanced distribution of electronic charges results in the formation of a more stable Si O Sr bond. For Sr-doped glasses, the well-formed Ca-P species would be transformed more quickly into an apatite layer, allowing for more Ca2+ substitutions within the newly formed apatite layer[10].

In the SiO2–CaO–SrO and SiO2–CaO–P2O5–SrO systems, strontium oxide-doped glasses have been studied [11, 12]. The interactions of bioactive glasses with biological fluids were investigated, and it was realized that strontium-containing glasses have a high potential for forming bone-like apatite [13-15 The exchange of alkali (Na) or alkaline (Ca2+) earth ions with H+ in the solution is usually linked to the bioactivity of glasses. This process causes silanol groups ((Si-OH) to condense, which is an important function that reacts readily with hydroxyl groups, carboxylic acids, and oxides found in inorganic compounds. In this case, the surface is distinguished by its large area. This silica gel layer contains or provides a large number of sites necessary for the formation and growth of hydroxycarbonate apatite species, which are similar to the mineral phase of bone[16].

The transition from highly bioactive glass to biocompatible compositions is marked by a significant increase in the silicate network's connectivity via Sr cation bonding, as well as an increase in the fraction of phosphate groups involved as P-O-Sr cross-links. Our findings also point to a strong correlation between the enhancement of crystalline apatite and the aggregation of Ca2+ and PO43- ions to form an apatite crystal structure that can be precipitated as a wallsotinte crystalline phase on CaSiO3. The process of thermal heat treatment is used as an effective route for crystallization enhancement in this situation [17, 18].

2. Materials and Methods

2.1 Sample preparation

An ordinary dissolve quenching technique was used to produce amorphous glasses within the system $xSrO-(45-x)SiO_2-24.5CaO-24.5Na_2O-6\ P_2O_5$, (0 x 15 mol %). Samples are obtained from reagent grade mixtures $CaCO_3$, Na_2CO_3, SiO_2, $SrCO_3$, and $(NH_4)_2HPO_4$ which have been melted in a Pt-Au crucible. To remove NH_3 and H_2O, The specimens were heat treated at a slow rate of 2°/min from room temperature to 600 °C, then melted for 20-30 minutes between 1000 and 1200 °C before being quenched by pouring the melt between two metallic plates. To restrict P_2O_5 volatilization and keep total glass weight losses under 2%, the time of melting and temperatures were optimized.

2.2 Infrared Spectra (IR)

The FTIR absorption spectroscopy for different samples were carried out by means of KBr pellets technique .The spectra are measured in the region of 400 - 4000 cm-1 with a spectral resolution of 2 cm using a Mattson 5000 FTIR spectrometer.[1] The obtained spectrum was normalized to the spectrum of blank KBr pellet and were corrected to the background and dark currents using two-point baseline correction.. The normalization is necessary to eliminate the concentration effect of the powder sample in the KBr disc.

2.3 X-ray diffraction spectroscopy

Shimadzu X-ray diffract meter is used for X-ray diffraction measurements (the apparatus type Dx-30, Metallurgy institute, El Tebbin-Cairo). The values of the maximum peak and intensity are used to determine the material type that compared to patterns in the joint committee for powder diffraction standards' international powder diffraction file (PDF) database (JCPDS).

2.4 Differential Scanning Calorimetry

A NETZSCH STA 409C/CD instrument was used to perform the DSC analysis. Crushed samples of known mass (30 mg) were put in an aluminum tray, sealed with a crimped lid, and heated at a rate of 5°C/min with argon as the carrier gas at a flow rate of 30 cm3 /min from 25°C to 1000°C.

2.5 Heat treatment (HT)

The samples containing 0, 3, 5,10 and 15 mol% SrO, were heated in a muffle furnace (Heraeus KR170) controlled within ± 2 °C. The samples were heat-treated at temperatures 500 and 650 °C for treatment time interval of 6 hours. After heating, the glasses were then kept into the furnace and held at the temperature of heat treatment for the desired time before cooling normally at room temperature.

2.6 Density and molar volume

The densities of the prepared samples were calculated using the Archimedes principle and benzene as the immersion solvent. The density was determined using the following formula:

$$\rho = \frac{W_a}{W_a - W_b} \times \rho_b \qquad (1)$$

where, W_a is the weight in air, W_b is the weight in benzene, and ρ_b is the density of benzene.
The molar volumes (V_m) were numerically determined using the equation that follows:

$$V_m = \frac{M_T}{\rho} \qquad (2)$$

where V_m is the molar volume. MT is the glass sample's molecular weight and ρ is the sample's density..

2.7 Micro hardness

The hardness value (Hv) of the prepared samples was determined using the SHIMADZU-HMV-G20S (Shimadzu, Kyoto, Japan) micro hardness tester at room temperature Ten indentations have been loaded at different places on the surface. The corresponding length of the indentation imprint diagonals registered by a high resolution microscope to ensure the accuracy of the measurement. The formula was used to calibrate the microhardness (Hv) values:

$$H_V = 1.854 \frac{F}{d^2} \qquad (3)$$

where Hv is the Vickers hardness in kg/mm2, F is the applied force in newtons, and d is the indentation's mean diagonal length in meters..

2.8 Magnetic Resonance Measurements

The JEOL GSX-500 high-resolution solid state MAS NMR spectrometer with a magnetic field of 11.74 T was used to analyses fine powdered samples of various

compositions (Mansoura University-EGYPT). . ^{31}P MAS NMR experiments were also conducted at resonance frequency (202.4 MHz) using a 3.2 mm diameter rotor spinning at 15 kHz. Solid NH4H2PO4 was used as a secondary reference compound and the signal from this set to 0.9 ppm. A pulse length of 2.5 μs and a recycle delay of 5 s was applied.

3 Results and Discussion

SrO gives the glasses good advantages toward improvements of their properties like extremely high resistant to thermal shock, high mechanical strength, good chemical stability, crystallinity and bioactivity [19]. It is evidenced from x-ray diffraction (XRD) and FTIR Figs. 1 & 2, of the as-prepared glasses that the well-formed structural species are constructed in its amorphous state [8,21]. The addition of SrO at expense of SiO_2 has no effect on the material structure, since the amorphous structure is the most dominant type, see figure 1, 2. From these figures, the spectral features do not changes upon increasing SrO contents. Because the glass composition has a limited effect, the thermal heat treatment processes can be applied as an alternative to change the material structure.

Figure 3 shows differential scanning calometr (DSC) curves from which both glass transition (Tg) and crystallization temperatures (T_C) can be determined. The crystallization temperature was ranged between 650^{O}C and 700^{O}C as is shown from figure 3. In addition, Tg is around 550^{O}C. According to DSC data, the glasses in the present study were all treated thermally at 500^{O}C and 650^{O}C for 6 hours. For example, treating the glass which contains 15 mol% SrO at 500^{O}C (curve b) can activate the nucleation process that leads to crystallization (curve c) when the glass treated at higher temperature (650C), see figure 4. The samples in such a case are simply crystallized which means that transformation into a more ordered structure occurred under the effect of thermal heat treatment and partially depends on the glass composition.

Comparisons of the studied materials' X-ray sharp diffraction line spectra with that of apatite ($Ca_3(PO_4)_2$) wollastonite ($CaSiO_3$) and [$Ca_2Sr\ (PO_4)_2$) crystals were considered. The most developed crystalline species are calcium phosphate, calcium silicate, and calcium strontium phosphate, according to the comparison [20]. The crystalline apatite and wollstonite formed species are considered the main units which play the role of

biocompatibility and or bioactivity of the studied materials [21, 22]. Figures 1, 4, and 5 of the XRD spectra indicate that the crystallization process is only available by thermal treatment. The number of diffraction lines in all investigating glasses is the same, but the most noticeable parameter is the change in intensities. This means that the well-formed crystalline phase types remain the same, but the content of the separated phases increases as SrO concentrations rise. Some well-formed crystalline phases, such as crystalline apatite (calcium phosphate crystals) and strontium calcium phosphate, are classified as bioactive phases that are beneficial to dental materials.[23, 24].

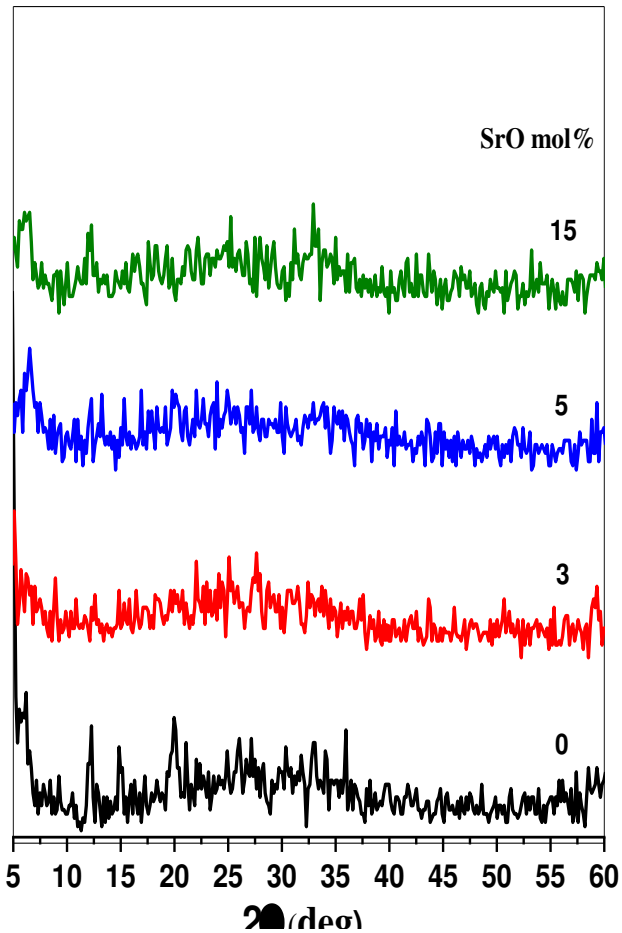

Figure 1 XRD spectra for as prepared glasses containing 0, 5, 10 and 15 mol% SrO.

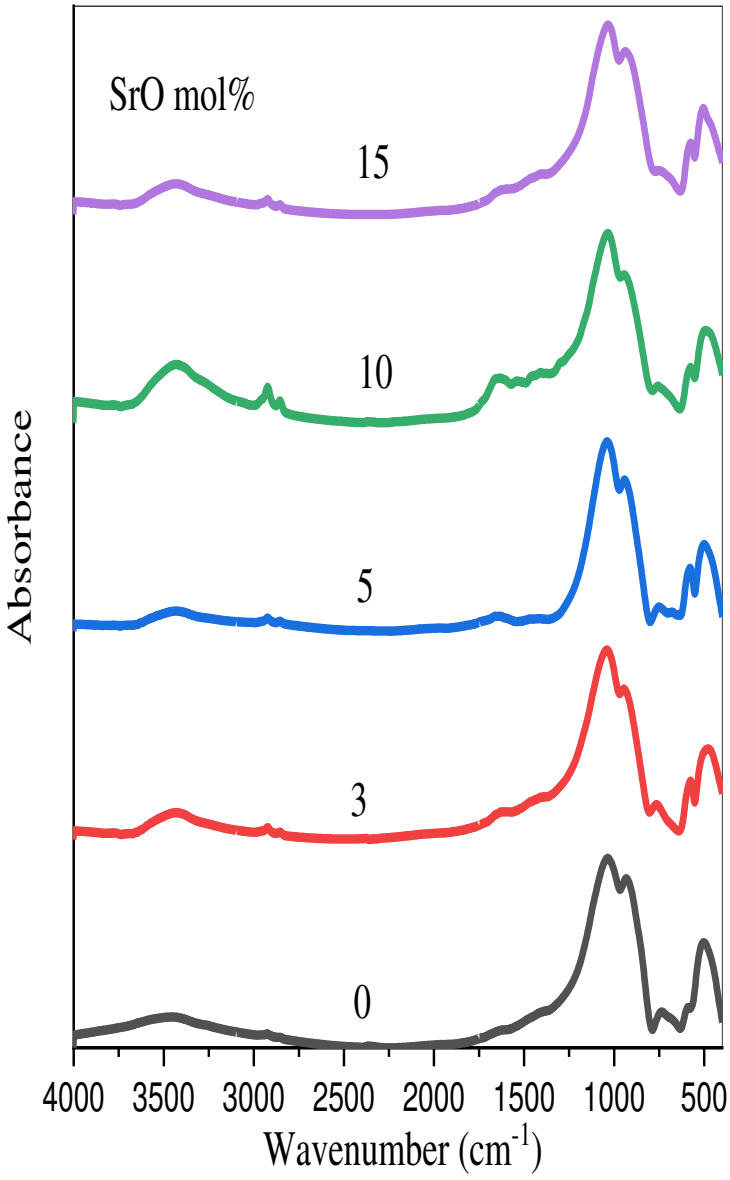

Figure 2 FTIR spectra for as prepared glasses containing 0, 5, 10 and 15 mol% SrO.

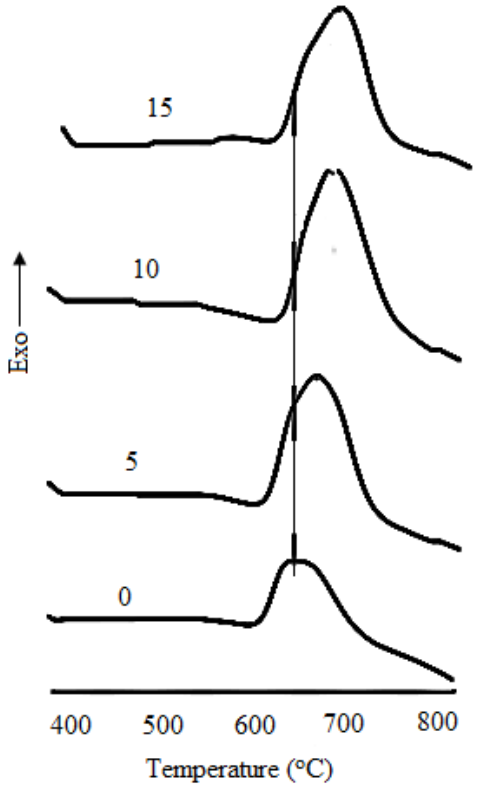

Figur3 DSC micrograph for sample containing 0,5,10 and 15 mol% SrO.

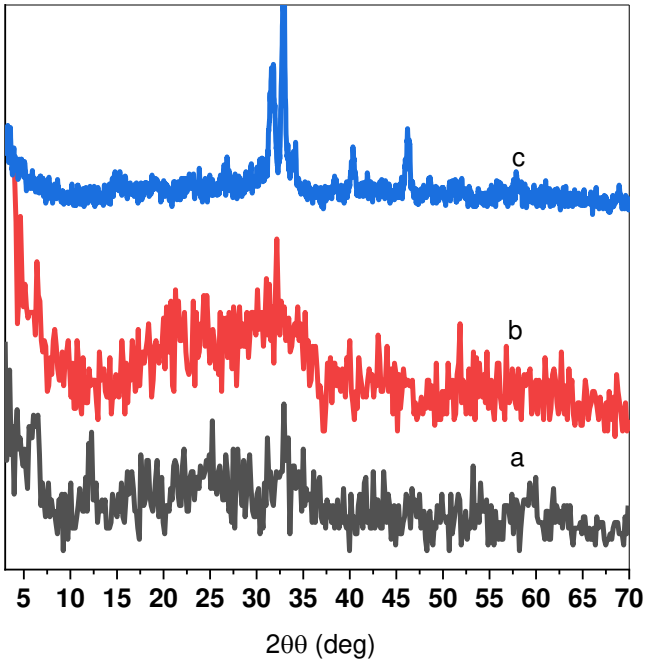

Figure 4 XRD for sample containing 5 mol% SrO, (a) as prepared, (b) treated at 500^0C treated and (c) trated at 650 C for 6 hours.

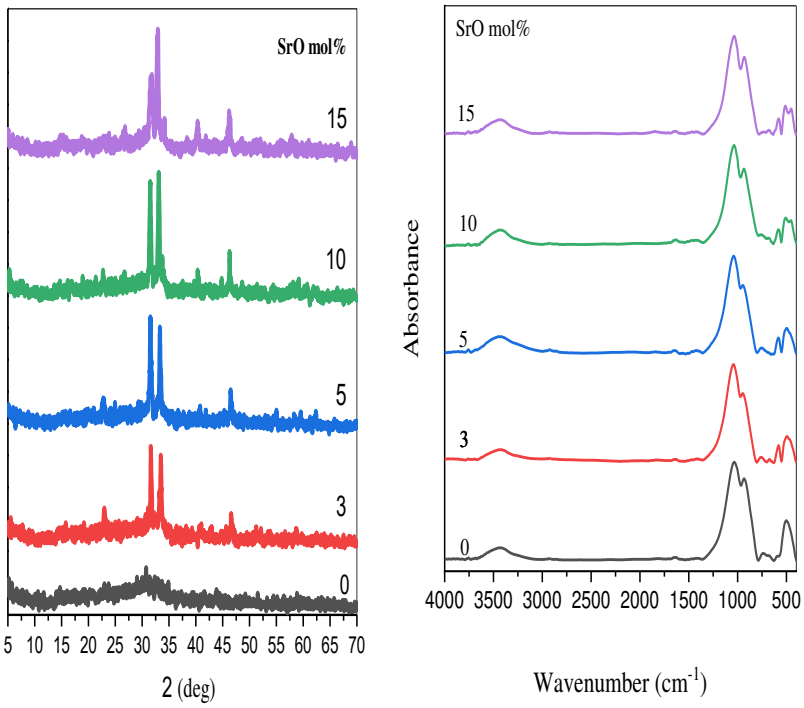

Figure 5 (a) XRD&(b) FTIR for sample containing different concentrations from SrO trated at 650 C for 6 hours

There is a clear difference between the FTIR spectra of as prepared abd treated samples, figure 2 and 5. The low frequency peaks between 400 and 600 al showed splitting in case of thermal treating cases. Such splitting in the absorption peaks lent support that both apatite and the wollastonite are formed in its crystalline phases. Which is confirmed by XRD figure 5. Then, in general, SrO in the matrix of the heat treated glasses modifies the silicate and phosphate structural units, forming wollastonite - apatite crystal phases and $Ca_2Sr\ (PO_4)_2$ apatite microcrystals [card no. 52-0467]. The latter type is more chemically stable against acid and fluid attack when it applied as a cements for oral applications.

Then from the above discussions, we conclude that increasing SrO leads to enhancing material crystallite of the treated glasses which in most cases enhances the mechanical properties.. Figure 6 shows the dependence of the hardness nimbler of the glasses on SrO content. Increasing the amounts of SrO enhances the hardness of the glasses which is changed from 280 kg/mm^{2}to 450Kg/mm^2.

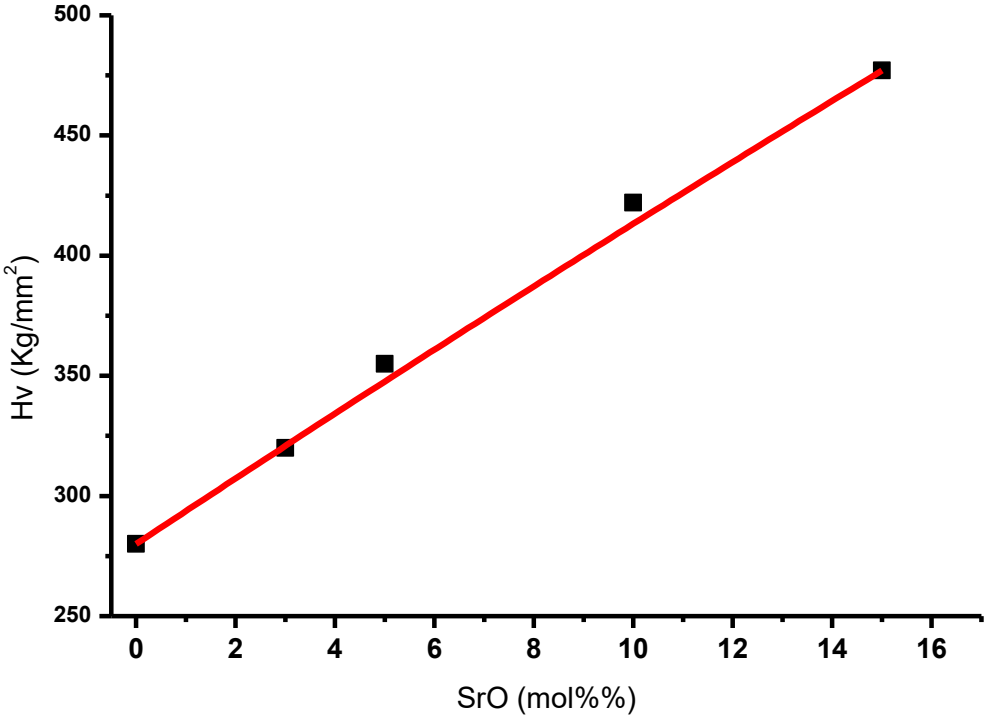

Figure 6 Change of hardness for sample containing different concentrations from SrO trated at 650 C for 6 hours

The change of XRD spectra and hardness number upon increasing SrO are considered due to modification of the apatit $Ca(PO_3)_2$ to involve Sr ions inducing $Ca_2Sr(PO_4)_2$ apatite one. Such species play the role in enhancing material hardness.

3.6 NMR Measurements

Figure 7 presents ^{31}P NMR spectra of different glasses containing 0, 5 and 15 mol% SrO which were all treated thermally at 650 for 6 hours. The phosphate units of Q^0 species (all oxygens are nonbridging) have been found in the main glass network indicating that the majority of phosphorus exists as orthophosphate species in the glass (Na_3PO_4 or $Ca_3(PO_4)_2$ or mixing between them)[25]. The change of the relative area of three spectra with SrO confirms the above consideration, since the relative area under the ^{31}PNMR spectra is increased by increasing SrO content that means that some of SrO my be forced to enter the apatite phase forming stransium apatie one. Then the apatite crystall shoud be formed from mixed cation (Ca and Sr) instesd of the one type (Ca) presnted by the lower area in figure 7 a.

Table 1 change of total area under the peak and SrO content

SrO (mol%)	Total area (cm2)
0	33
5	64
15	95

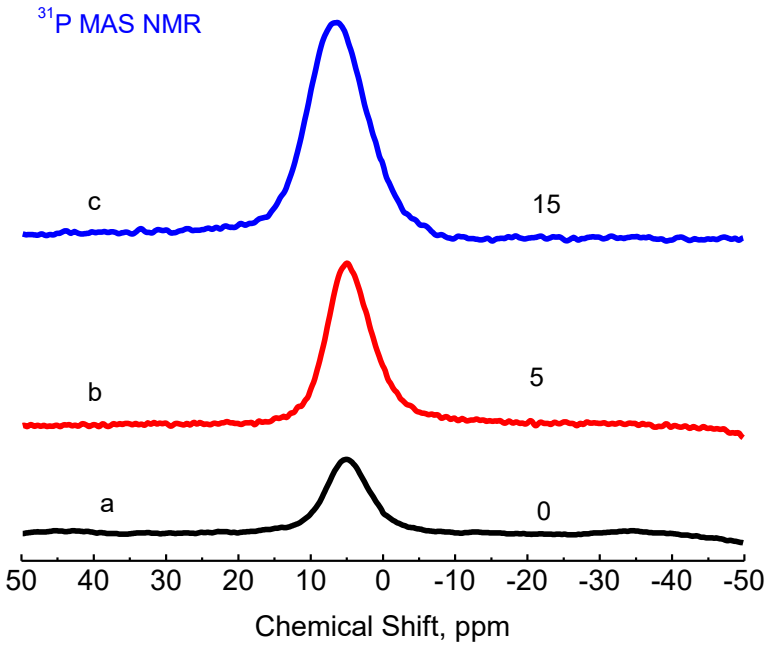

Figure7 ^{31}P NMR spectra for glasses containing different SrO concentration and treated at 650 for 6 hours.

The clear difference between ^{23} NMR spectra of glasses of 0 and 15 mol % SrO figure 8 support the vesion that Sr can substiute both Na or Ca from the apatite phase and some of Sr can shair in performing the apatite crystalline phases. From figure 8, the chemical shift of Na nuclei of the glasses containing Sr is lower than that of Sr free glass. This means that bond strength in network structure of glasses

containing Sr is stronger than that of Sr free ones.

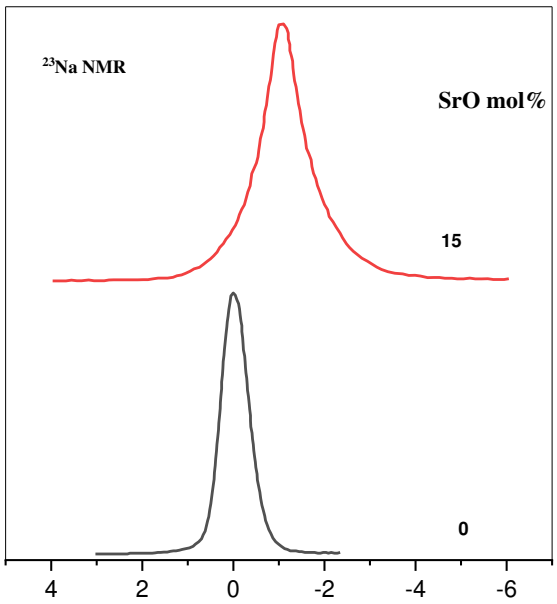

Figure 8 ^{23}Na NMR spectra for glasses containing different SrO concentration.

3.7 Density and molar volume measurements

Changes of both density (D) and molar volume (Vm) with increasing SrO concentration are presented in Fig. 9. The density increased and its molar volume decreased as the content of SrO is increased from 0 to 15 mol%. The observed icreased in density values is mainly due to higher molecular weight of SrO (103.62 g/mol) when it compared with that of SiO_2 (60.09g/mol). Accordingly, with increasing SrO content, SrO enters gradually the network as a glass forming species which leads to increasing the total bridging bonds at the expense of non-bridging ones (Sr-O-Si) . As a consequence, formation of shortening Sr–O–P linkages is considered the main reason for the well-decreased volume of the network structure [30]. The decreasing in NBO is accompanied with decreasing the open volume and void spaces surrounded NBO ions which in all cases results in decreasing the molar volume of the studied glass.

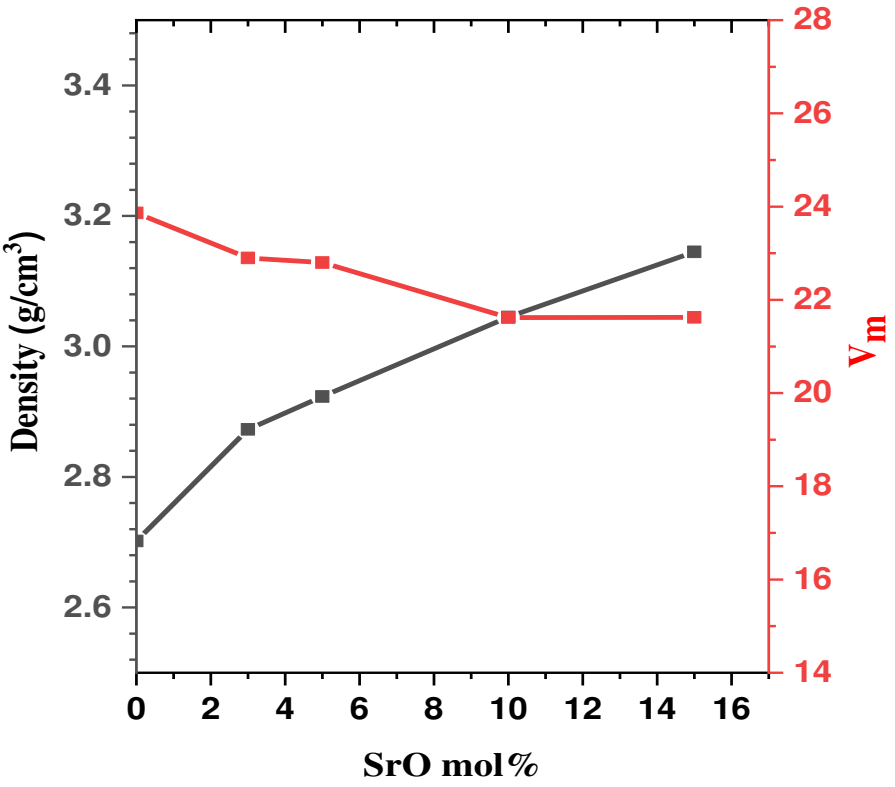

Figure9: The Density and molar volume as function of SrO content (mol %)

4. Conclusion

Bioglasses and glass ceramics containing different SrO concentrations have been studied by different structural techniques. Amorphous nature of the glass free from SrO is confirmed by XRD. Some types of crystalline species are formed in SrO containing glasses after heat treatment. Well-formed apatite ($Ca_3(PO_4)_2$) , wollastonite ($CaSiO_3$) and [Ca_2Sr $(PO_4)_2$) phases containing strontium ions are evidenced in SrO containing glasses. More enhancement in crystallinity was confirmed via thermal heat treatment process. Presence of Sr ions in both crystalline apatite and wollastonite matrix promotes its biocompatibility, particularly orthopedic bioactivity.

Authors declarations

- Ethics approval and consent to participate: The authors agree to the Echics approval and consent to participate.
- Consent for publication: We all authors agree to publish this work in Silicon
- Availability of data and material. We declare that the data and materials are available
- Disclosure of potential conflicts of interest: We all authors declare that there is no conflict of interest between us.
- Competing interests : There is no any competing interests. The authors did not receive support from any organization for the submitted work

- **Financial interests:** The authors declare they have no financial interests
- **Authorship clarified:** All authors agreed with the content and that all gave explicit consent to submit.
- Authors' contribution: All authors whose names appear on the submission made substantial contributions to the conception or design of the work; and analysis, of data. Material preparation, and data analysis were performed by {Gomaa El Damrawi and Rawia Mohmoud Ramadan}. Data collection is performed by Mohamed Biomy. The first draft of the manuscript was written by [Gomaa El Damrawi] and all authors commented on previous versions of the manuscript. All authors read and approved the final manuscript.

5. References

1. Lao, J., J.-M. Nedelec, and E. Jallot, *New strontium-based bioactive glasses: physicochemical reactivity and delivering capability of biologically active dissolution products.* Journal of Materials Chemistry, 2009. **19**(19): p. 2940-2949.
2. Ogueri, K.S., et al., *Polymeric biomaterials for scaffold-based bone regenerative engineering.* Regenerative engineering and translational medicine, 2019. **5**(2): p. 128-154.
3. Kaur, G., et al., *A review of bioactive glasses: their structure, properties, fabrication and apatite formation.* Journal of Biomedical Materials Research Part A: An Official Journal of The Society for Biomaterials, The Japanese Society for Biomaterials, and The Australian Society for Biomaterials and the Korean Society for Biomaterials, 2014. **102**(1): p. 254-274.
4. Fernandes, H.R., et al., *Bioactive glasses and glass-ceramics for healthcare applications in bone regeneration and tissue engineering.* Materials, 2018. **11**(12): p. 2530.
5. O'Neill, E., et al., *The roles of ions on bone regeneration.* Drug discovery today, 2018. **23**(4): p. 879-890.
6. Lao, J., E. Jallot, and J.-M. Nedelec, *Strontium-delivering glasses with enhanced bioactivity: a new biomaterial for antiosteoporotic applications?* Chemistry of Materials, 2008. **20**(15): p. 4969-4973.
7. Zhou, Y., C. Wu, and J. Chang, *Bioceramics to regulate stem cells and their microenvironment for tissue regeneration.* Materials Today, 2019. **24**: p. 41-56.
8. Al-Qaysi, M., *Development of Phosphate Based Glass Scaffolds for the Repair of Craniofacial Bone*. 2018, UCL (University College London).
9. Deshmukh, K., et al., *Recent advances and future perspectives of sol–gel derived porous bioactive glasses: a review.* RSC Advances, 2020. **10**(56): p. 33782-33835.
10. Bee, S.-L. and Z.A. Hamid, *Hydroxyapatite derived from food industry bio-wastes: Syntheses, properties and its potential multifunctional applications.* Ceramics International, 2020.
11. Salman, S., S. Salama, and H. Abo-Mosallam, *The role of strontium and potassium on crystallization and bioactivity of Na2O–CaO–P2O5–SiO2 glasses.* Ceramics International, 2012. **38**(1): p. 55-63.
12. Massera, J. and L. Hupa, *Influence of SrO substitution for CaO on the properties of bioactive glass S53P4.* Journal of Materials Science: Materials in Medicine, 2014. **25**(3): p. 657-668.
13. Wu, C., et al., *Strontium-containing mesoporous bioactive glass scaffolds with improved osteogenic/cementogenic differentiation of periodontal ligament cells for periodontal tissue engineering.* Acta Biomaterialia, 2012. **8**(10): p. 3805-3815.
14. Zhang, J., et al., *Three-dimensional printing of strontium-containing mesoporous bioactive glass scaffolds for bone regeneration.* Acta biomaterialia, 2014. **10**(5): p. 2269-2281.

15. Kargozar, S., et al., *Synthesis, physico-chemical and biological characterization of strontium and cobalt substituted bioactive glasses for bone tissue engineering.* Journal of Non-Crystalline Solids, 2016. **449**: p. 133-140.
16. Erasmus, E.P.-I., *Synthesis, testing and characterization of porous biocompatible porous bioactive glasses for clinical use.* PhD diss, 2017.
17. Brauer, D.S., *Bioactive glasses—structure and properties.* Angewandte Chemie International Edition, 2015. **54**(14): p. 4160-4181.
18. Eckert, H., *Structural characterization of bioactive glasses by solid state NMR.* Journal of Sol-Gel Science and Technology, 2018. **88**(2): p. 263-295.
19. Mysen, B.O. and P. Richet, *Silicate glasses and melts*. 2018: Elsevier.
20. Duminis, T., S. Shahid, and R.G. Hill, *Apatite glass-ceramics: a review.* Frontiers in Materials, 2017. **3**: p. 59.
21. El-Damrawi, G., et al., *Structural Investigations on Na2O–CaO-V2O5-SiO2 Bioglass Ceramics.* Current Journal of Applied Science and Technology, 2016: p. 1-9.
22. Kenny, S. and M. Buggy, *Bone cements and fillers: a review.* Journal of Materials Science: Materials in Medicine, 2003. **14**(11): p. 923-938.
23. Gómez-Morales, J., et al., *Progress on the preparation of nanocrystalline apatites and surface characterization: Overview of fundamental and applied aspects.* Progress in Crystal Growth and Characterization of Materials, 2013. **59**(1): p. 1-46.
24. Irfan, M. and M. Irfan, *Overview of hydroxyapatite; composition, structure, synthesis methods and its biomedical uses.* Biomedical Letters, 2020. **6**(1): p. 17-22.
25. Ahmed, I., et al., *Comparison of phosphate-based glasses in the range 50P2O5–(50− x) CaO–xNa2O prepared using different precursors.* Glass Technology-European Journal of Glass Science and Technology Part A, 2008. **49**(2): p. 63-72.

Figures

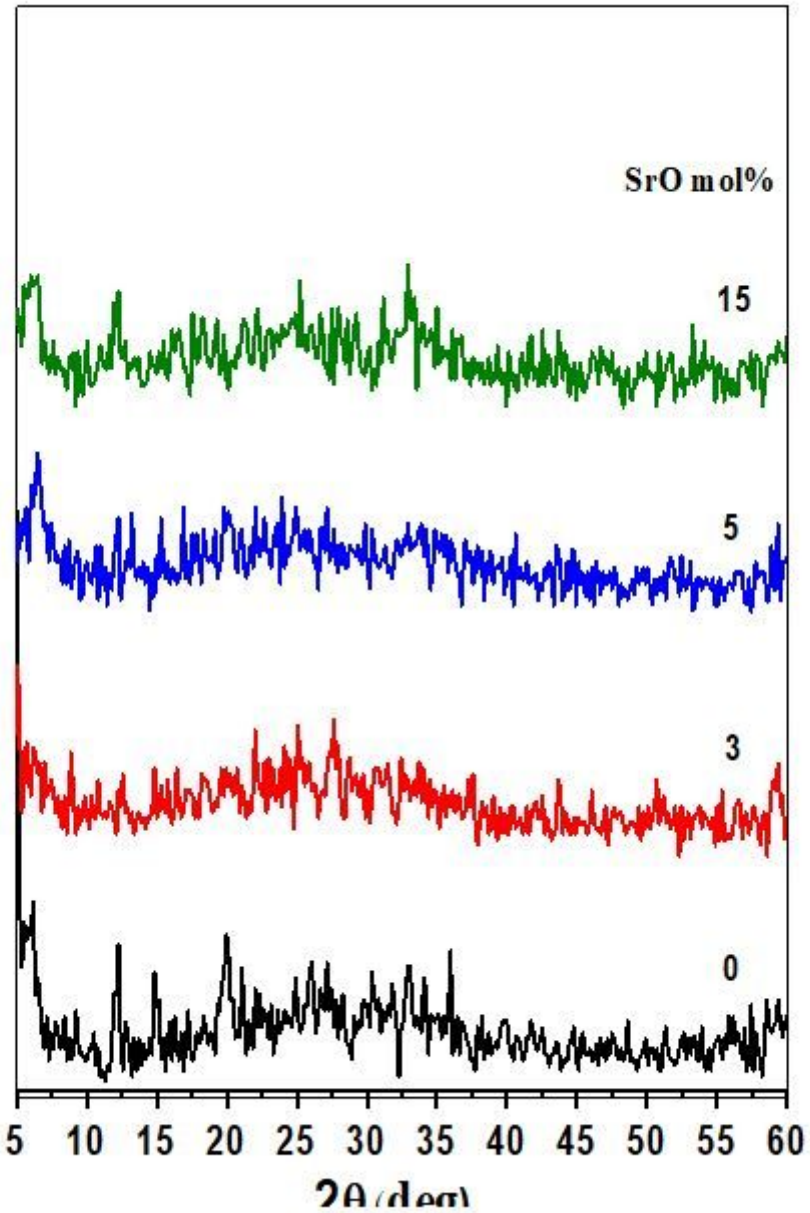

Figure 1

XRD spectra for as prepared glasses containing 0, 5, 10 and 15 mol% SrO.

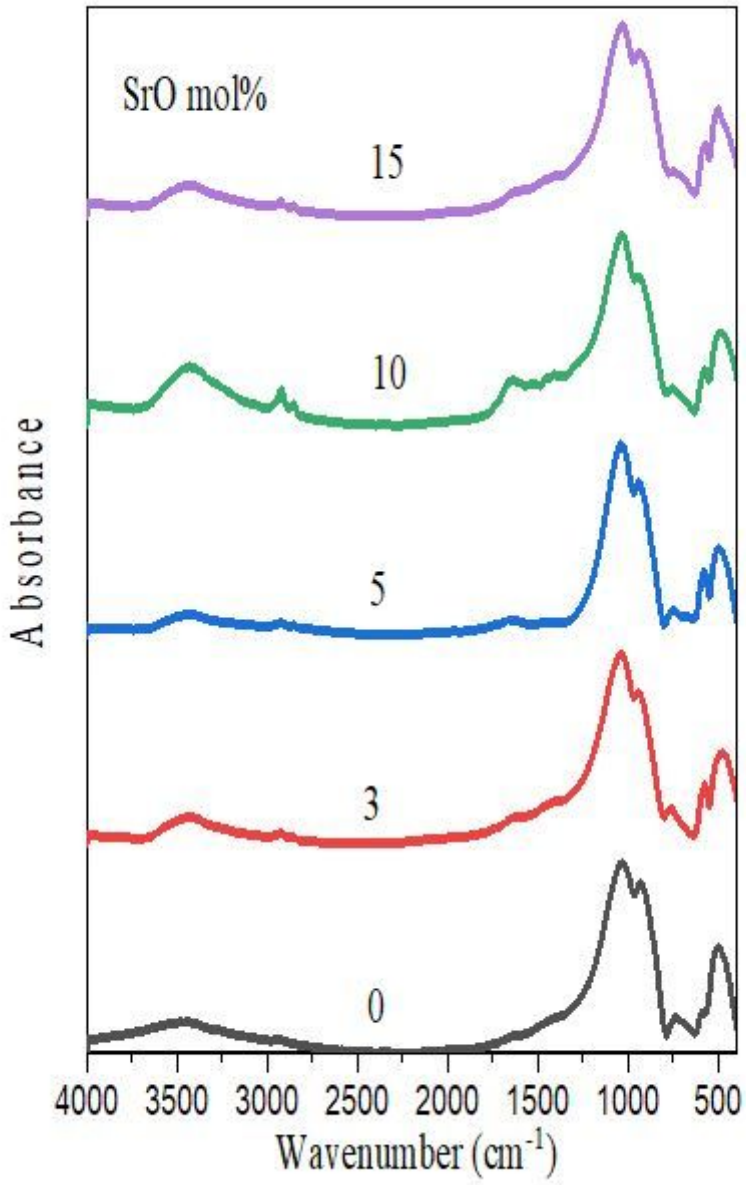

Figure 2

FTIR spectra for as prepared glasses containing 0, 5, 10 and 15 mol% SrO.

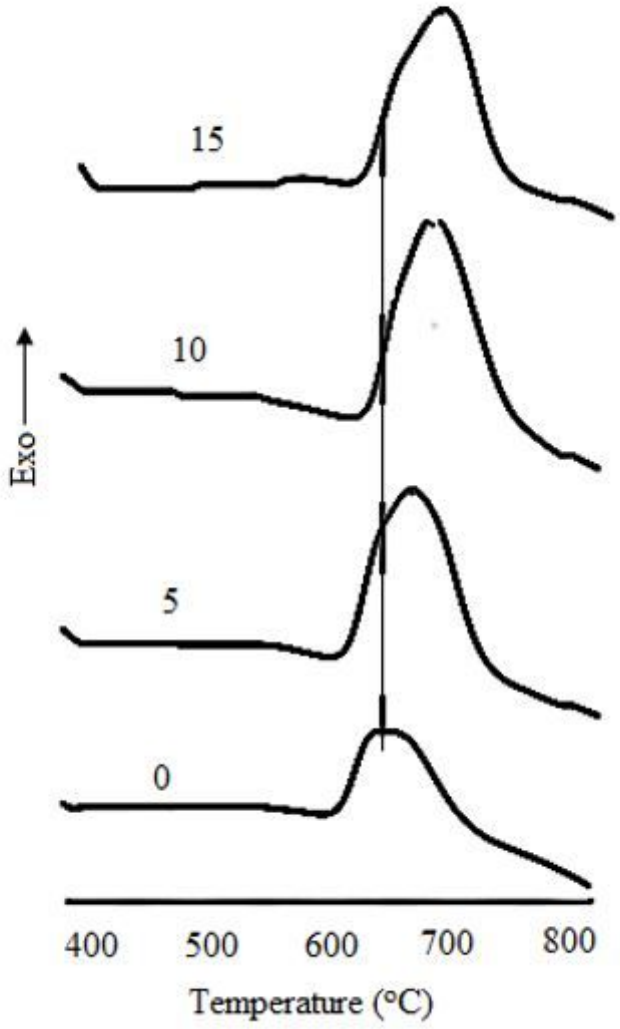

Figure 3

DSC micrograph for sample containing 0,5,10 and 15 mol% SrO.

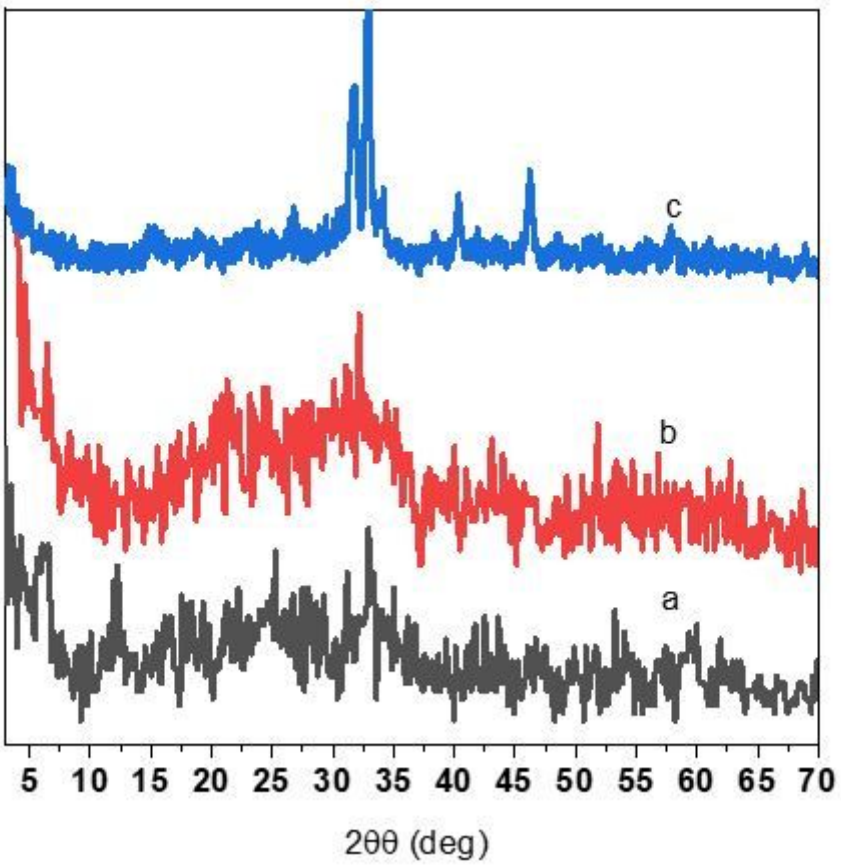

Figure 4

XRD for sample containing 5 mol% SrO, (a) as prepared, (b) treated at 5000C treated and (c) trated at 650 C for 6 hours.

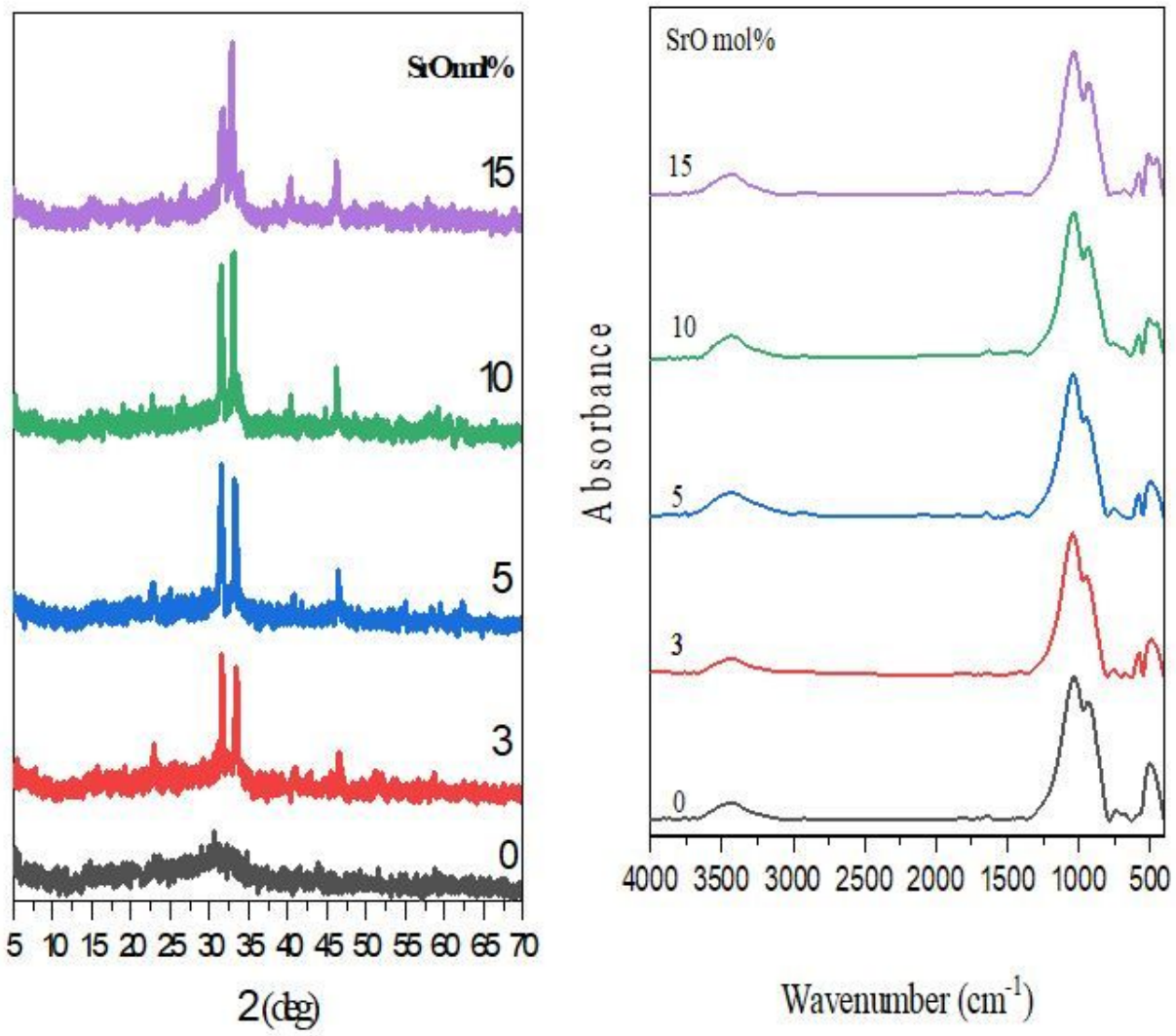

Figure 5

(a) XRD&(b) FTIR for sample containing different concentrations from SrO trated at 650 C for 6 hours

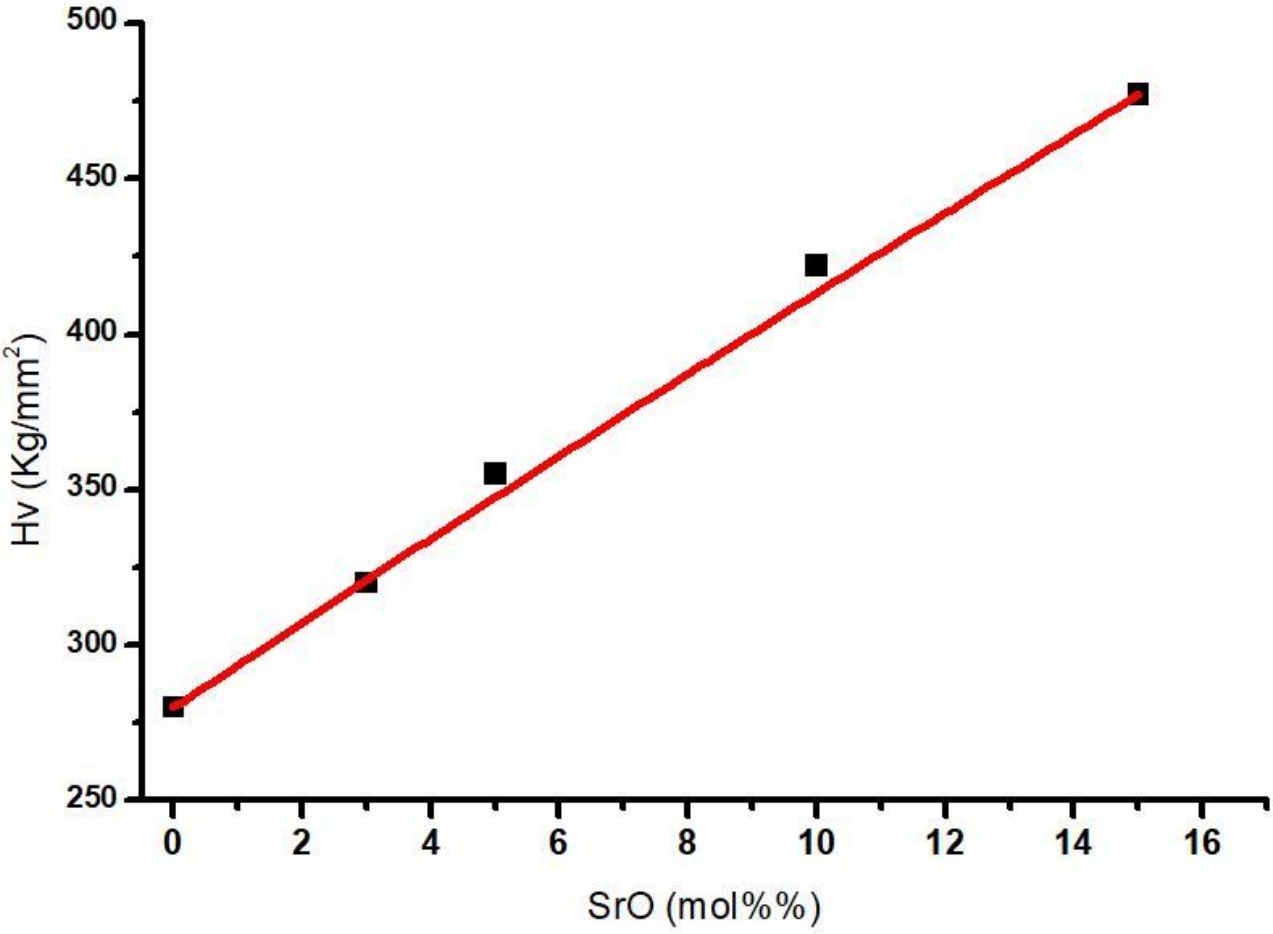

Figure 6

Change of hardness for sample containing different concentrations from SrO trated at 650 C for 6 hours

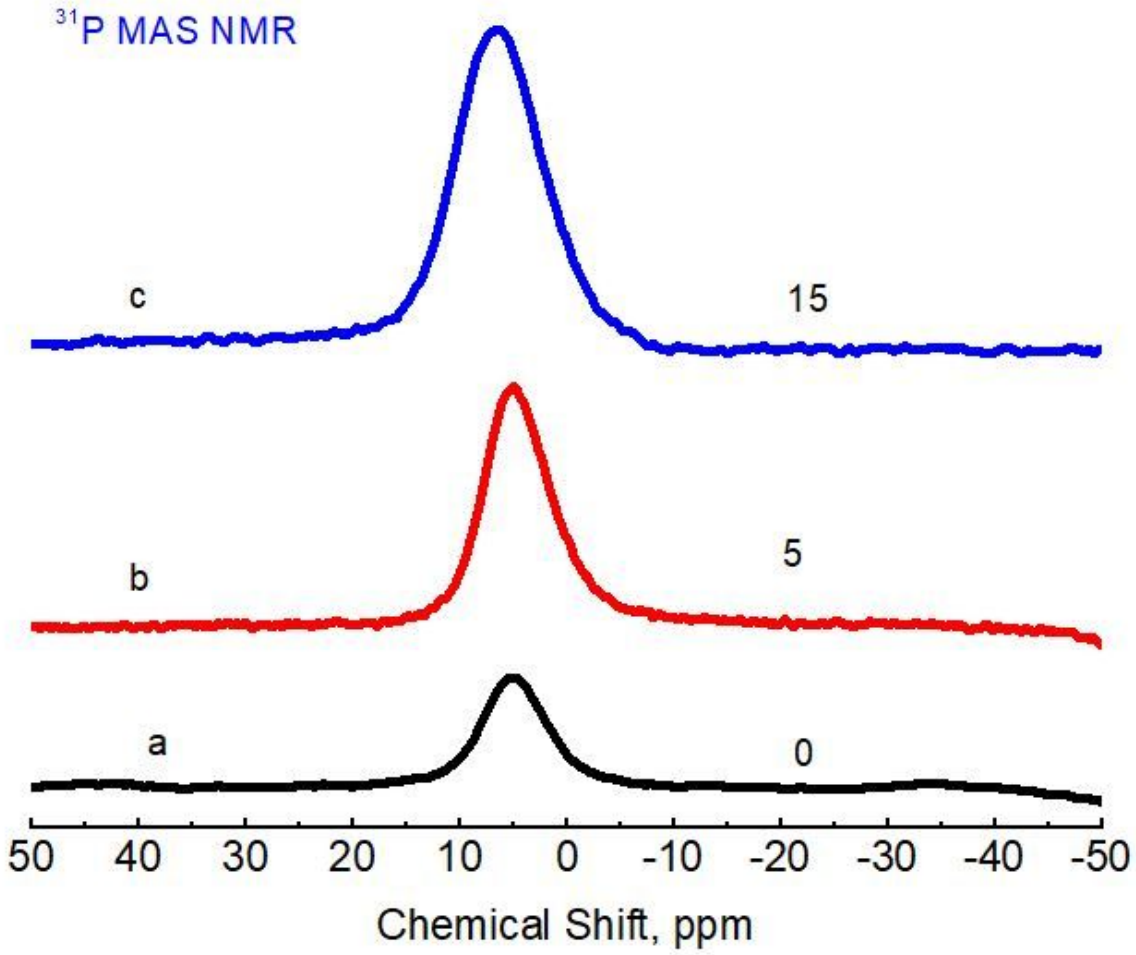

Figure 7

31P NMR spectra for glasses containing different SrO concentration and treated at 650 for 6 hours.

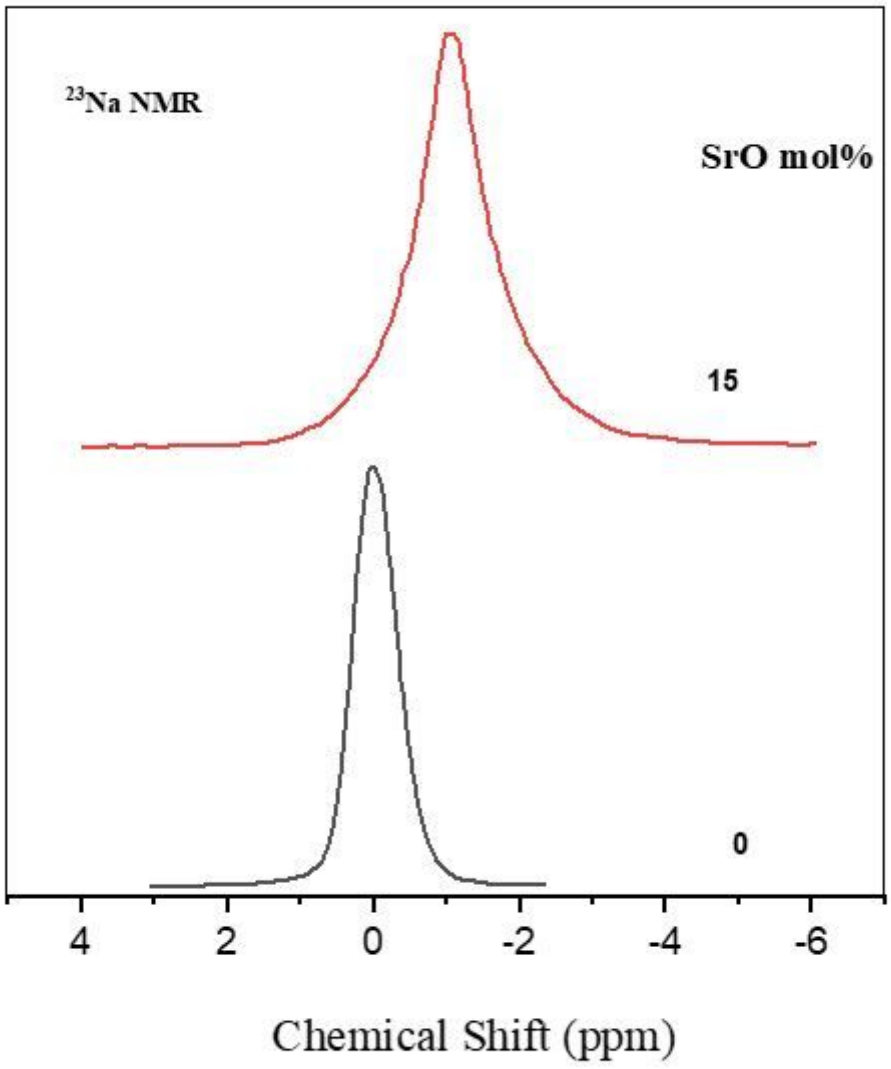

Figure 8

23Na NMR spectra for glasses containing different SrO concentration.

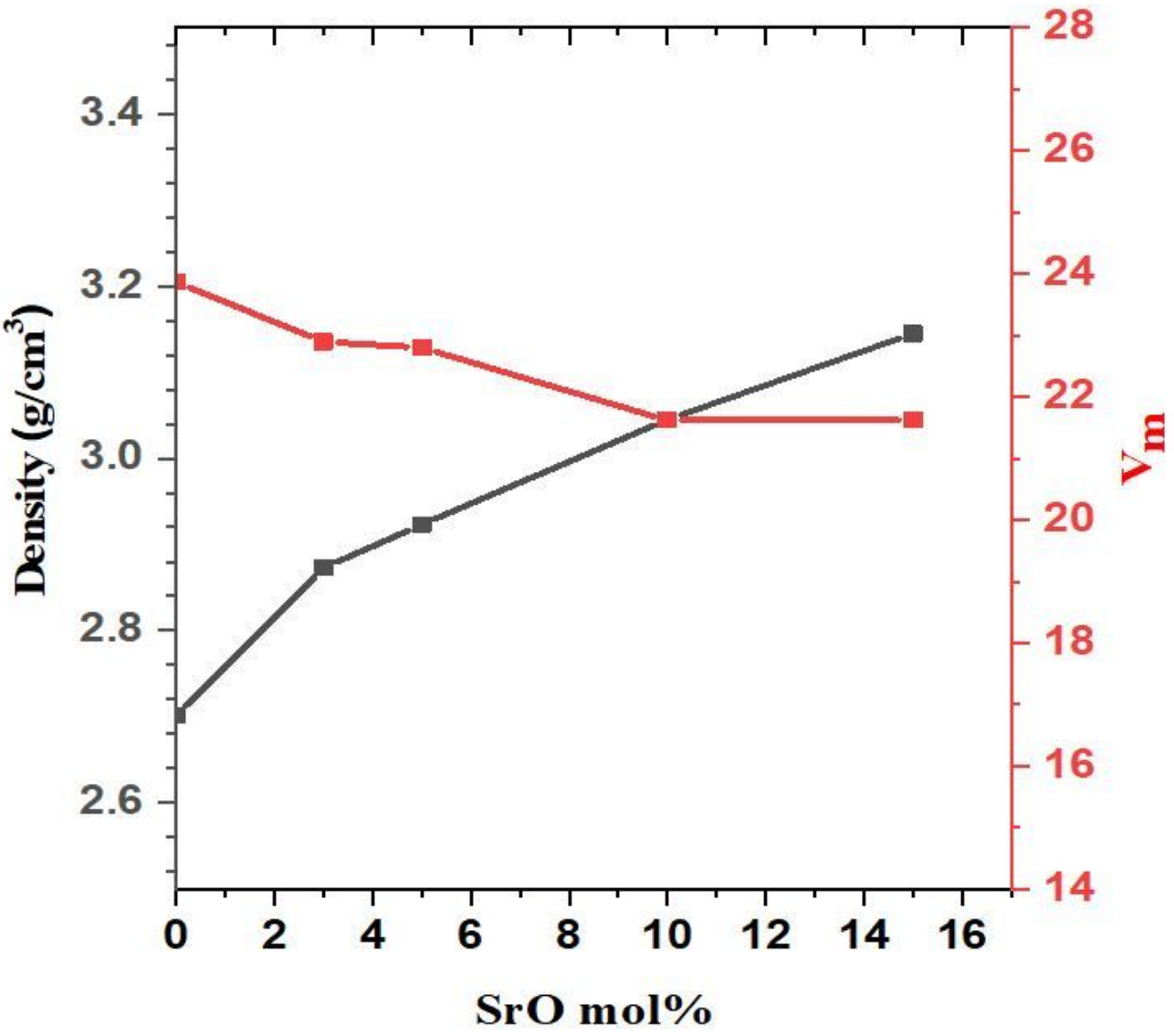

Figure 9

The Density and molar volume as function of SrO content (mol %)